Supporting Information

Discovery and Structural Optimization of N5-Substituted 6,7-dioxo-6,7-dihydropteridines as Potent and Selective Epidermal Growth Factor Receptor (EGFR) Inhibitors Against L858R/T790M Resistance Mutation

Yongjia Hao[1, #], Xia Wang[1,#], Tao Zhang[2,#], Deheng Sun[1], Yi Tong[1], Yuqiong Xu[1], Haiyang Chen[1], Linjiang Tong[2], Lili Zhu[1], Zhenjiang Zhao[1], Zhuo Chen[1], Jian Ding[2], Hua Xie[2,*], Yufang Xu,[1,*] and Honglin Li[1,*]

[1]Shanghai Key Laboratory of New Drug Design, Shanghai Key Laboratory of Chemical Biology, State Key Laboratory of Bioreactor Engineering, School of Pharmacy, East China University of Science & Technology, Shanghai 200237, China; [2]Division of Anti-tumor Pharmacology, State Key Laboratory of Drug Research, Shanghai Institute of Materia Medica, Chinese Academy of Sciences, Shanghai, 201203, China.

*To whom correspondence should be addressed. Email: hxie@jding.dhs.org, yfxu@ecust.edu.cn, hlli@ecust.edu.cn

Content

Superposition simulations S2

Docking studies S2

Binding mode analysis S3

In vivo antitumor efficacy study S4

Material and methods of kinase assay S4

General preparation of the key intermediates 15f-j. S5

NMR spectra S8

REFERENCES S22

Superposition simulations

We did molecular superposition simulations for compound **9** and the designed inhibitors (**17a-e**) by a fast 3D molecular similarity calculation algorithm, SHAFTS[1]. All compounds were stored in a 2D SDF file and an original conformation would be generated for each compound, then a conformation generation program based on a multi-objective evolution algorithm, Cyndi[2], was used to generate the conformation ensembles (a maximum size of 200 conformers) for each compound. The template structure was the crystal conformation of compound **4** bound to the ATP-binding site of $EGFR^{T790M}$ with the PDB code of 3IKA[3]. Then SHAFTS would do the molecular fitting considering the shape overlay and pharmacophore features to build more valid models. The entire calculation process was simply performed submitting a job to the ChemMapper[4] server, and the structures and SHAFTS similarity scores for all the compounds can be accessed at the same online site using the job ID of 38880 (http://lilab.ecust.edu.cn/chemmapper/result/getResult.html?jobId=38880).

Docking studies

Glide docking. The X-ray structures of $EGFR^{WT}$ (PDB 4G5J)[5] and $EGFR^{T790M}$ (PDB 3IKA) were initially used in docking studies. All EGFR structures were retrieved from the Protein Data Bank and the molecular docking was performed with Glide[6] (Schrödinger, Inc., version 9.0) in extra precision (XP) mode. The designed compounds (**17c-e**) were first docked into the EGFR protein as a reversible inhibitor using Glide, which was applied following the next steps:

1) All water molecules were removed from the structure of the complex. Hydrogen atoms and charges were added during a brief relaxation that was performed using the "Protein Preparation Wizard" workflow. After optimizing the hydrogen bond network, the crystal structure was minimized using the OPLS_2005 force field with the maximum root mean square deviation (RMSD) value of 0.3 Å.
2) The grid-enclosing box was placed on the centroid of compound **4** in the optimized crystal structure as described above, and defined so as to enclose residues located within 20 Å around the ATP-binding site, and a scale factor of 1.0 was set to van der Waals (VDW) radii of those receptor atoms with the partial atomic charge less than 0.25.
3) The three ligands were prepared with LigPrep module in Maestro, including adding hydrogen atoms, ionizing at a pH range from 5.0 to 9.0, and generating stereoisomers and valid single 3D conformers.
4) XP approach of Glide was adopted to dock the molecules into the ATP-binding site with the default parameters, and the top-ranking poses of each molecule were retained.

Covalent bond formation. One of the best poses was chosen based on the distance and orientation of the electrophilic functional group for each compound.

Consequently, the covalent bond between the sulfur atom on the Cys797 thiol and the terminal carbon atom on the acrylamide group was formed, and the bond geometry was optimized through the minimization using OPLS_2005 with MacroModel module in Maestro. The default values of the optimization parameters and thresholds were kept. All torsion angles of compound were released to freely rotate. The modeling structure of $EGFR^{T790M}$ was overlaid with the $EGFR^{WT}$ structure using PyMol, and all the structures are saved in the form of PDB coordinate files with names beginning with PDB code and ending with compound No., such as "*3IKA_complexed_with_17d.pdb*".

Binding mode analysis

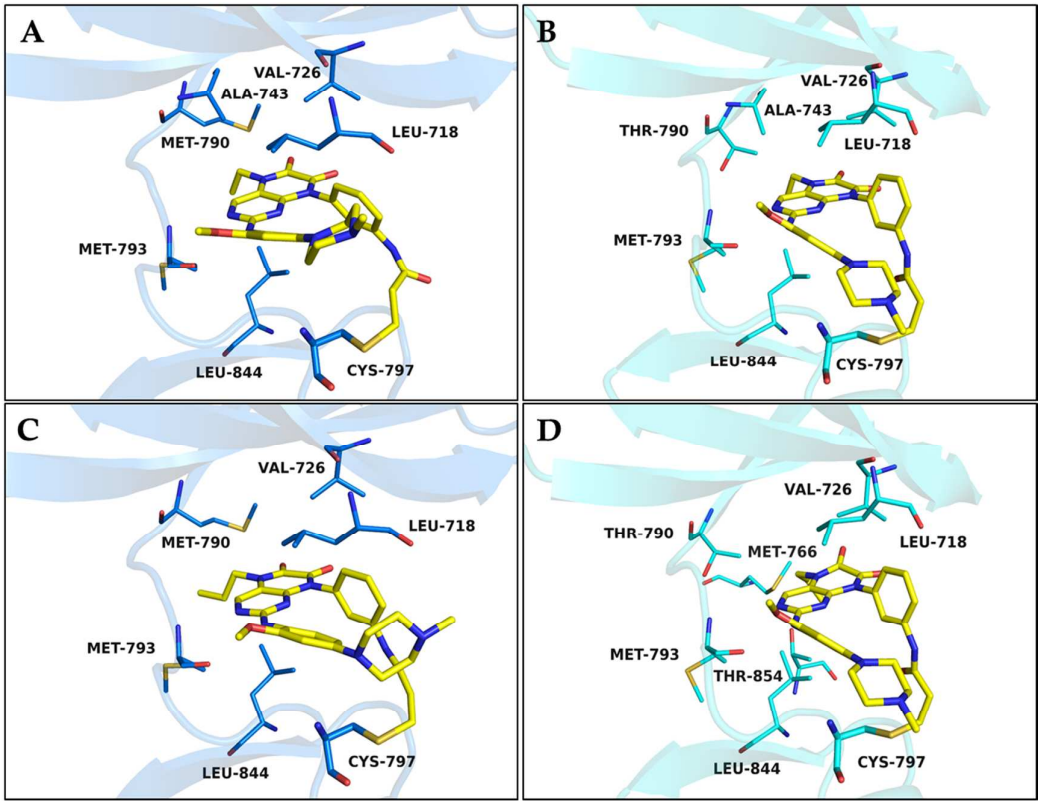

Figure S1. Structural modeling of compounds **17c** (A) and **17e** (C) bound to $EGFR^{T790M}$ (PDB 3IKA) in the ATP-binding site. Predicted poses of compounds **17c** (B) and **17e** (D) against $EGFR^{WT}$ (PDB 4G5J).

In vivo antitumor efficacy study

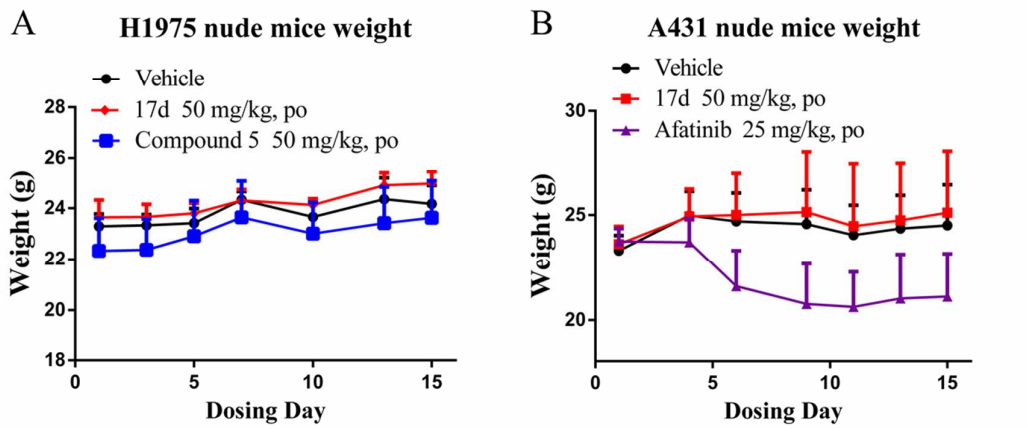

Figure S2. Preliminary *in vivo* antitumor efficacy of **17d**. (A) Body weights of H1975 xenograft mouse model (n = 3), (B) body weights of A431 xenograft mouse model (n = 6). All values represent mean ± SEM.

Material and methods of kinase assay

Kinases domain of $EGFR^{WT}$, $EGFR^{L858R/T790M}$ were expressed using the Bac-to-Bac™ baculovirusexpression system (Invitrogen, Carlsbad, CA, USA) and purified in Ni-NTA columns (QIAGEN Inc., Valencia, CA, USA). The kinase activity was evaluated with enzyme-linked immunosorbent assay (ELISA). Briefly, 20 μg/mL Poly ($_{Glu, Tyr}$) 4:1 (Sigma, St. Louis, MO) was precoated in 96-well ELISA plates as substrate. Added 50 μL of 10 μmol/L ATP solution which was diluted in kinase reaction buffer (50 mM HEPES pH7.4, 20 mM $MgCl_2$, 0.1 mM $MnCl_2$, 0.2 mM Na_3VO_4, 1 mM DTT), the plate was treated with 1μL of indicated concentrations of compounds (dissolved in DMSO) per well. Experiments at each concentration were performed in duplicate. Reaction was initiated by adding tyrosine kinase diluted in kinase reaction buffer. After incubation at 37°C for 1 h, the wells were washed three times with phosphate buffered saline (PBS) containing 0.1% Tween 20 (T-PBS). 100 μL anti-phosphotyrosine (PY99) antibody (1:1000, Santa Cruz Biotechnology, Santa Cruz, CA) diluted in T-PBS containing 5 mg/mL BSA was added and the plate was incubated at 37°C for 30 min. After the plate was washed three times, 100 μL horseradish peroxidase-conjugated goat anti-mouse IgG (1:2000, Calbiochem, SanDiego, CA) was added and the plate was incubated at 37°C for 30 min. The plate was washed, added with 100 μL citrate buffer (0.1 M, pH 5.5) containing 0.03% H_2O_2 .Then 2 mg/mL o-phenylenediamine was added, and samples were incubated at room temperature until color emerged. The reaction was terminated immediately by adding 50 μL of 2M H_2SO_4 . Plate was read using a multiwell spectrophotometer (VERSAmax™, Molecular Devices, Sunnyvale, CA, USA) at 492 nm. The inhibitory

rate (%) was calculated with the formula: [1–(A_{492} treated/A_{492} control)]×100%. IC_{50} values were calculated from the inhibitory curves.

General preparation of the key intermediates 15f-j.

The following compounds **15f-j** were prepared by a method similar to that for compound **15**.

***tert*-butyl(3-(2-((4-((2-(dimethylamino)ethyl)(methyl)amino)-2-methoxyphenyl)amino)-6,7-dioxo-6,7-dihydropteridin-8(5*H*)-yl)phenyl)carbamate (15f)**

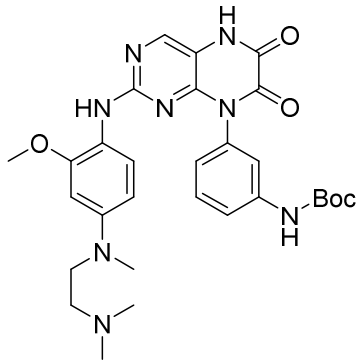

^{1}H NMR (400 MHz, DMSO-d_6) δ 9.61 (s, 1H), 8.12 (s, 1H), 7.57 (s, 1H), 7.54-7.52 (m, 1H), 7.41 (t, J = 8.0 Hz, 1H), 7.18 (d, J = 8.8 Hz, 1H), 6.95 (d, J = 8.0 Hz, 1H), 6.26 (d, J = 2.4 Hz, 1H), 5.86 (d, J = 7.6 Hz, 1H), 3.75 (s, 3H), 2.84 (s, 3H), 2.49 (t, J = 7.2 Hz, 2H), 2.24 (t, J = 7.2 Hz, 2H), 2.19 (s, 6H), 1.45 (s, 9H). LC-MS: m/z: 577.4 $(M+H)^+$.

***tert*-butyl(3-(2-((4-(2-(dimethylamino)ethoxy)-2-methoxyphenyl)amino)-6,7-dioxo-6,7-dihydropteridin-8(5*H*)-yl)phenyl)carbamate (15g)**

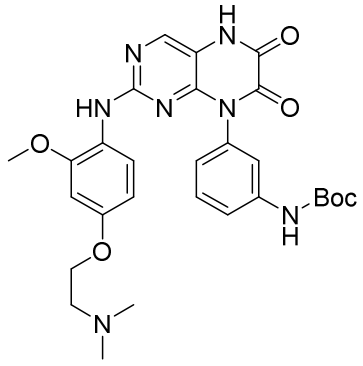

^{1}H NMR (400 MHz, DMSO-d_6) δ 9.64 (s, 1H), 8.15 (s, 1H), 7.63-7.61 (m, 2H), 7.52 (d, J = 8.0 Hz, 1H), 7.44 (t, J = 8.0 Hz, 1H), 7.31 (d, J = 8.8 Hz, 1H), 6.96 (d, J = 7.2 Hz, 1H), 6.53 (s, 1H), 6.08 (d, J = 8.8 Hz, 1H), 3.96 (t, J = 7.2 Hz, 2H), 3.77 (s, 3H), 2.59 (t, J = 7.2 Hz, 2H), 2.22 (s, 6H), 1.45 (s, 9H). LC-MS: m/z: 564.3 $(M+H)^+$.

***tert*-butyl(3-(2-((2-methoxy-4-(4-(4-methylpiperazin-1-yl)piperidin-1-yl)phenyl)amino)-6,7-dioxo-6,7-dihydropteridin-8(*5H*)-yl)phenyl)carbamate (15h)**

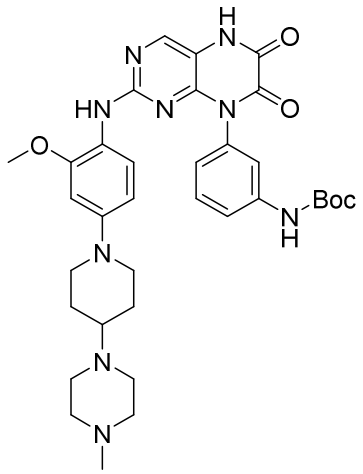

^{1}H NMR (400 MHz, DMSO-d_6) δ 9.64 (s, 1H), 8.15 (s, 1H), 7.58-7.56 (m, 2H), 7.55 (s, 1H), 7.43 (t, J = 8.0 Hz, 1H), 7.25 (d, J = 8.8 Hz, 1H), 6.95 (d, J = 7.6 Hz, 1H), 6.52 (d, J = 2.0 Hz, 1H), 6.07 (d, J = 8.8 Hz, 1H), 3.76 (s, 3H), 3.59-3.56 (m, 2H), 3.45-3.41 (m, 4H), 2.58-2.53 (m, 6H), 2.34-2.32 (m, 2H), 2.25 (s, 3H), 1.83 (d, J = 11.2 Hz, 2H), 1.54-1.49 (m, 1H), 1.46 (s, 9H). LC-MS: m/z: 658.5 $(M+H)^+$.

***tert*-butyl(3-(2-((3-methyl-4-(4-methylpiperazin-1-yl)phenyl)amino)-6,7-dioxo-6,7-dihydropteridin-8(5*H*)-yl)phenyl)carbamate (15i)**

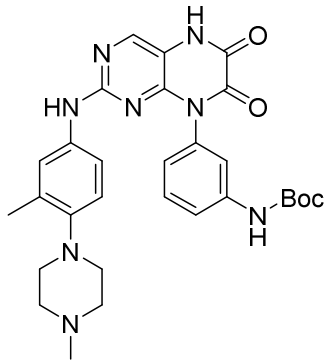

^{1}H NMR (400 MHz, DMSO-d_6) δ 9.64 (s, 1H), 9.29 (s, 1H), 8.18 (s, 1H), 7.60 (s, 1H), 7.54 (d, J = 6.4 Hz, 1H), 7.44 (t, J = 7.2 Hz, 1H), 7.08 (s, 1H), 7.05-7.03 (m, 1H), 6.95 (d, J = 4.4 Hz, 1H), 6.66 (d, J = 7.6 Hz, 1H), 2.70 (t, J = 4.0 Hz, 4H), 2.43 (t, J = 4.0 Hz, 4H), 2.22 (s, 3H), 1.99 (s, 3H), 1.45 (s, 9H). LC-MS: m/z: 559.3 $(M+H)^+$.

***tert*-butyl(3-(2-((3-methoxy-4-(4-methylpiperazin-1-yl)phenyl)amino)-6,7-dioxo-6,7-dihydropteridin-8(5*H*)-yl)phenyl)carbamate (15j)**

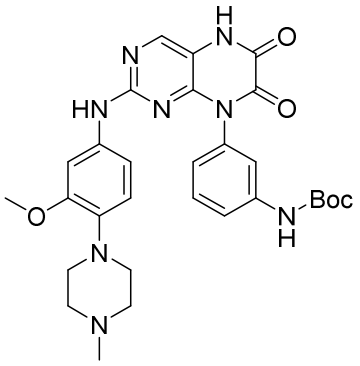

^{1}H NMR (400 MHz, DMSO-d_6) δ 9.64 (s, 1H), 9.23 (s, 1H), 8.19 (s, 1H), 7.60 (s, 1H), 7.54 (d, J = 6.0 Hz, 1H), 7.43 (t, J = 7.6 Hz, 1H), 6.94 (t, J = 6.4 Hz, 1H), 6.87 (s, 1H), 6.45 (d, J = 7.2 Hz, 1H), 3.59 (s, 3H), 2.83 (t, J = 4.0 Hz, 4H), 2.42 (t, J = 4.0 Hz, 4H), 2.21 (s, 3H), 1.45 (s, 9H). LC-MS: m/z: 575.3 $(M+H)^+$.

The 2D HMBC spectrum of compound 16c.
***tert*-butyl(3-(5-ethyl-2-((2-methoxy-4-(4-methylpiperazin-1-yl)phenyl)amino)-6,7-dioxo-6,7-dihydropteridin-8(5*H*)-yl)phenyl)carbamate (16c).**

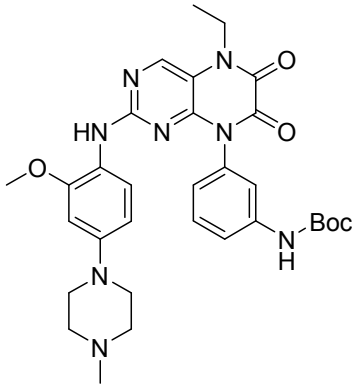

^{1}H NMR (500 MHz, DMSO-d_6) δ 9.68 (s, 1H), 8.54 (s, 1H), 7.69 (s, 1H), 7.65 (s, 1H), 7.60 (d, J = 6.4 Hz, 1H), 7.49 (t, J = 6.4 Hz, 1H), 7.30 (d, J = 6.8 Hz, 1H), 7.00 (d, J = 6.4 Hz, 1H), 6.61 (s, 1H), 6.12 (d, J = 6.0 Hz, 1H), 4.18 (q, J = 5.2 Hz, 2H), 3.82 (s, 3H), 3.19 (t, J = 4.4 Hz, 4H), 2.88 (t, J = 4.4 Hz, 4H), 2.54 (s, 3H), 1.49 (s, 9H), 1.30 (t, J = 5.6 Hz, 3H). ^{13}C NMR (125 MHz, DMSO-d_6) δ 155.52, 154.59, 152.72, 152.65, 148.97, 147.14, 146.10, 143.59, 140.58, 135.97, 129.33, 120.04, 121.29, 119.38, 118.04, 113.67, 106.63, 100.16, 79.27, 55.77, 53.73, 47.78, 44.25, 36.85, 28.11, 21.08, 12.00. HRMS(ESI) (m/z): $(M+H)^+$ calcd for $C_{31}H_{39}N_8O_5$ 603.3043, found, 603.3047. The obtained 2D HMBC spectrum was shown in Figure S3, which was consistent with the description in the reference.[7]

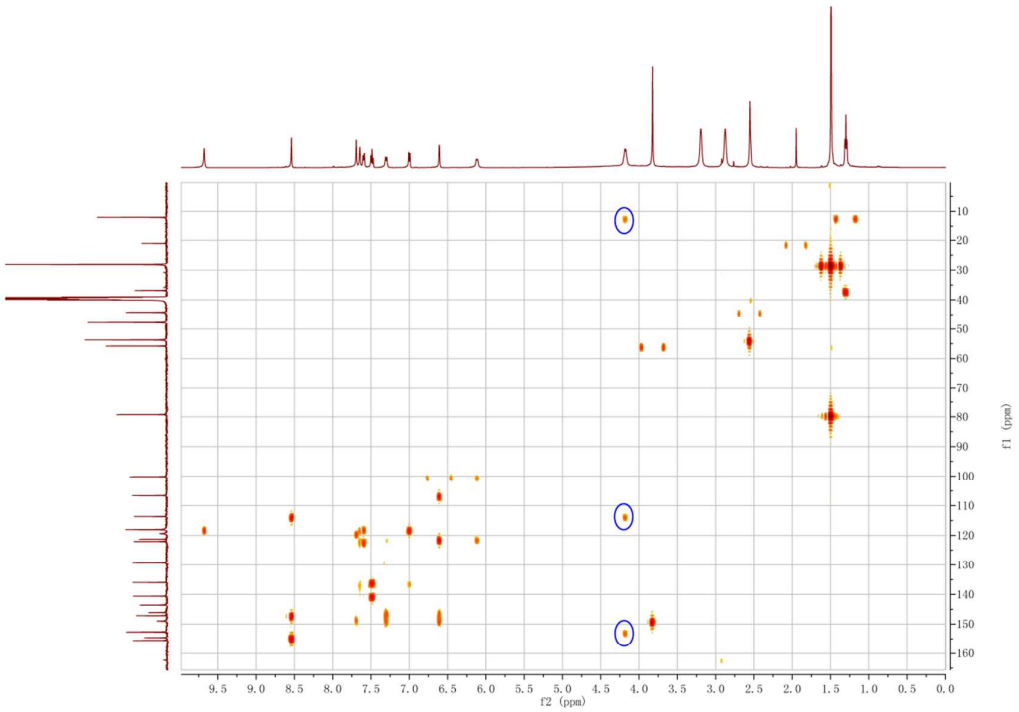

Figure S3. The 2D HMBC NMR spectrum of compound **16c**.

NMR spectra

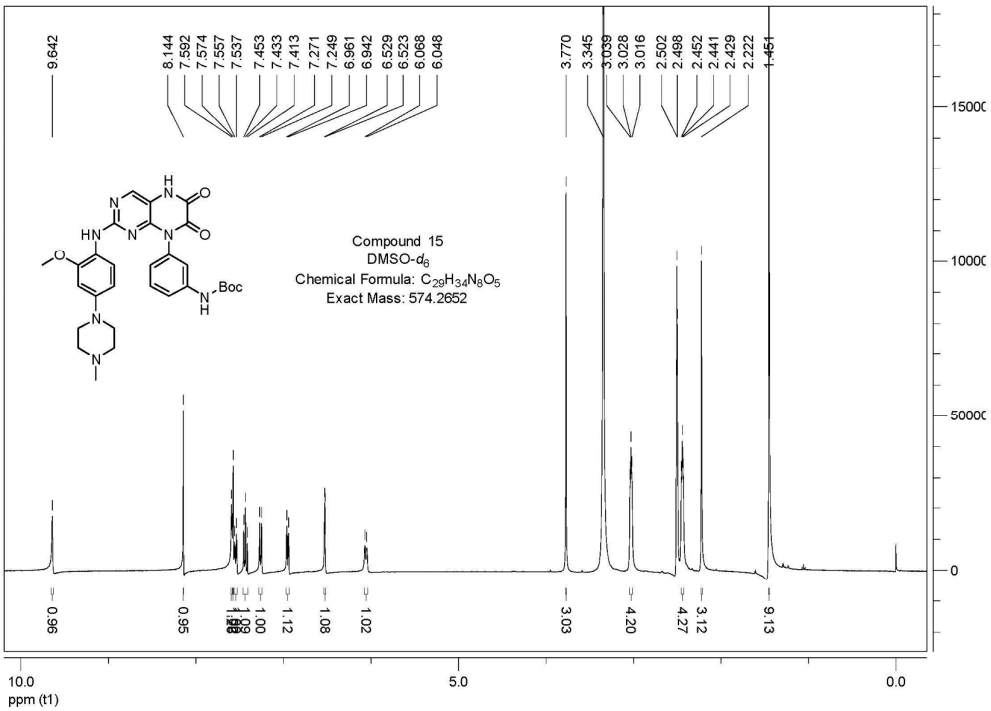

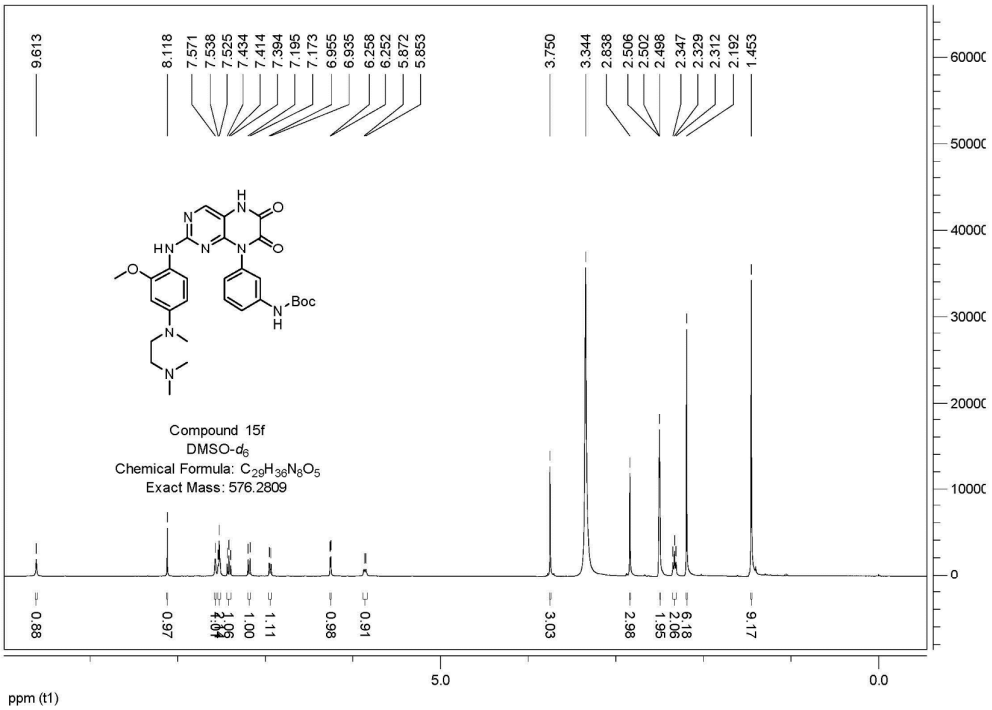
9.613
8.118
7.571
7.538
7.525
7.434
7.414
7.394
7.195
7.173
6.955
6.935
6.258
6.252
5.872
5.853
3.750
3.344
2.838
2.506
2.502
2.498
2.347
2.329
2.312
2.192
1.453
Boc
Compound 15f
DMSO-d_6
Chemical Formula: $C_{29}H_{36}N_8O_5$
Exact Mass: 576.2809
0.88
0.97
1.00
1.11
0.98
0.91
3.03
2.98
1.95
2.06
6.18
9.17
5.0
0.0
ppm (t1)

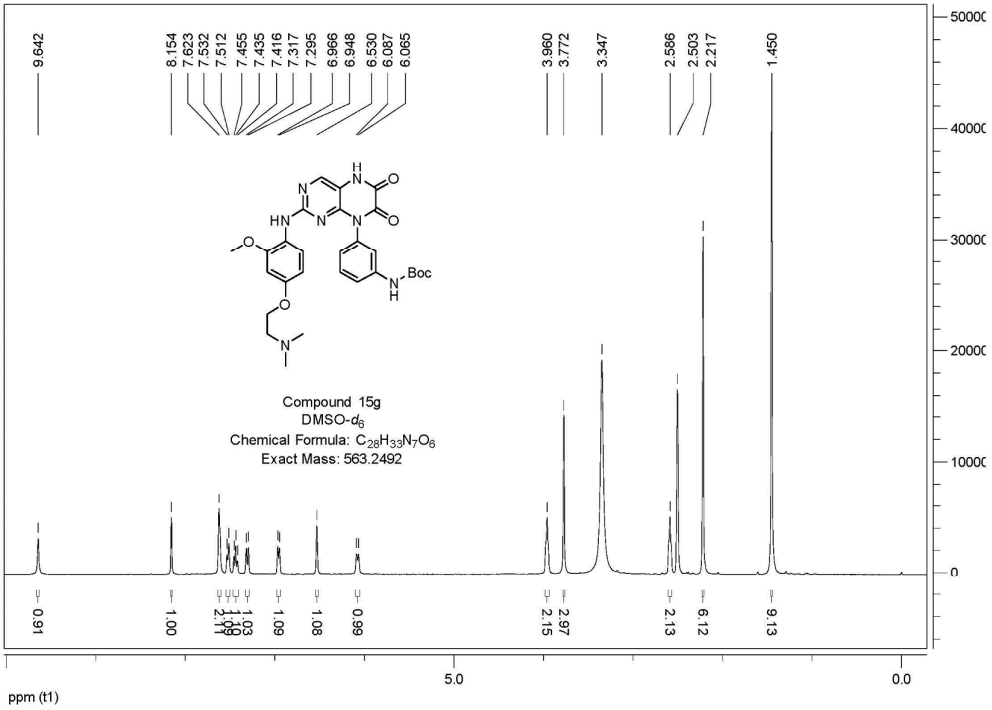
9.642
8.154
7.623
7.532
7.512
7.455
7.435
7.416
7.317
7.295
6.966
6.948
6.530
6.087
6.065
3.960
3.772
3.347
2.586
2.503
2.217
1.450
Boc
Compound 15g
DMSO-d_6
Chemical Formula: $C_{28}H_{33}N_7O_6$
Exact Mass: 563.2492
0.91
1.00
2.11
1.03
1.09
1.08
0.99
2.15
2.97
2.13
6.12
9.13
5.0
0.0
ppm (t1)

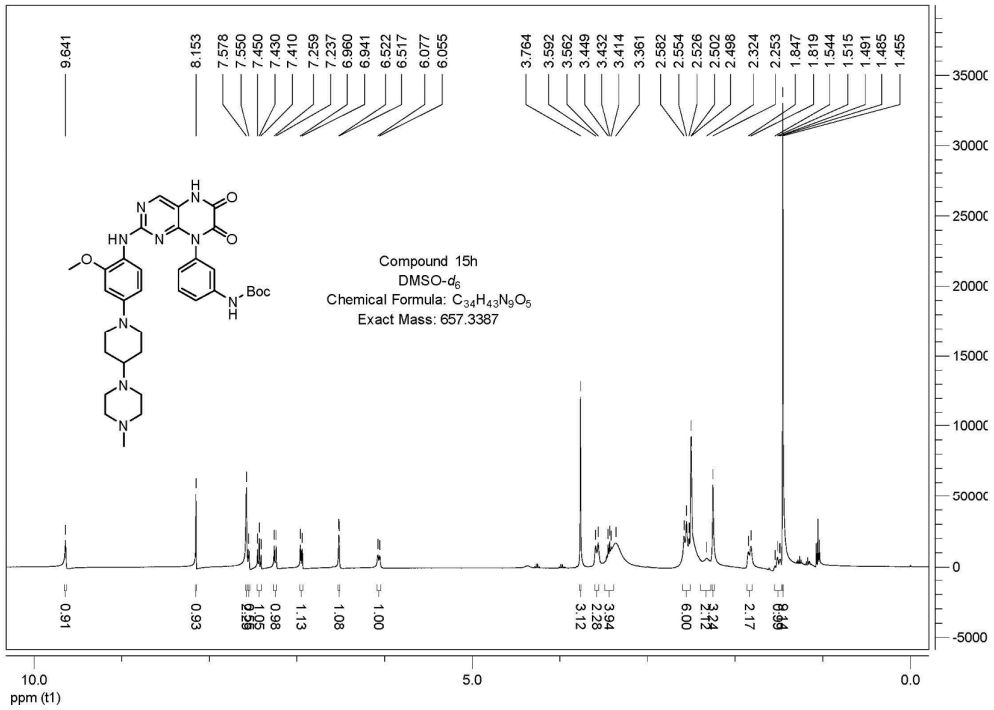
Compound 15h
DMSO-d_6
Chemical Formula: $C_{34}H_{43}N_9O_5$
Exact Mass: 657.3387
ppm (t1)

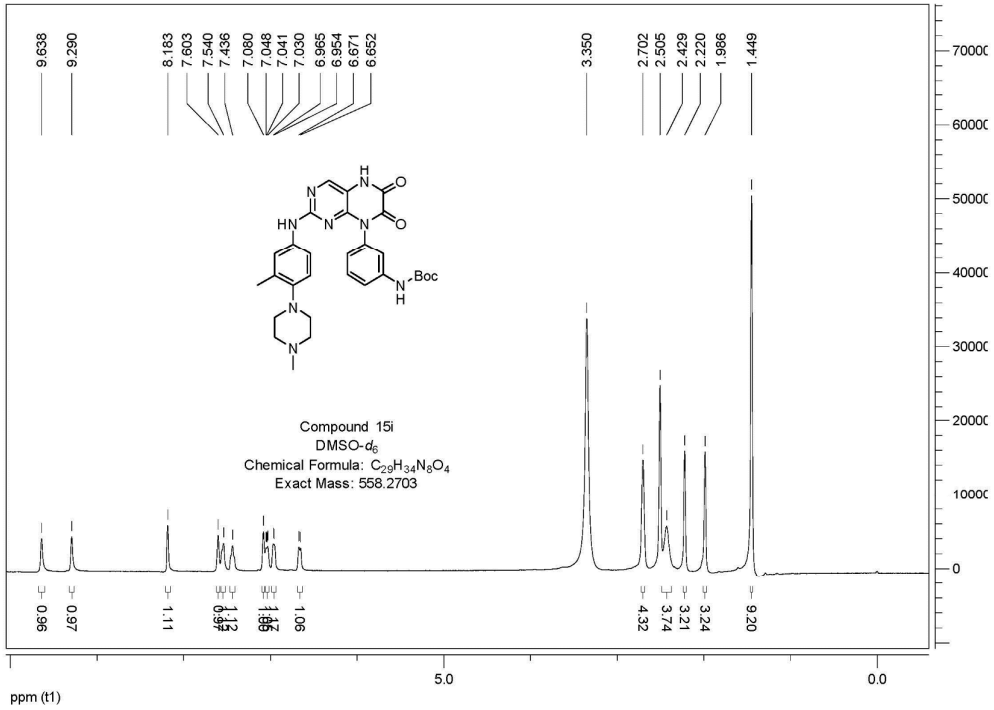
Compound 15i
DMSO-d_6
Chemical Formula: $C_{29}H_{34}N_8O_4$
Exact Mass: 558.2703
ppm (t1)

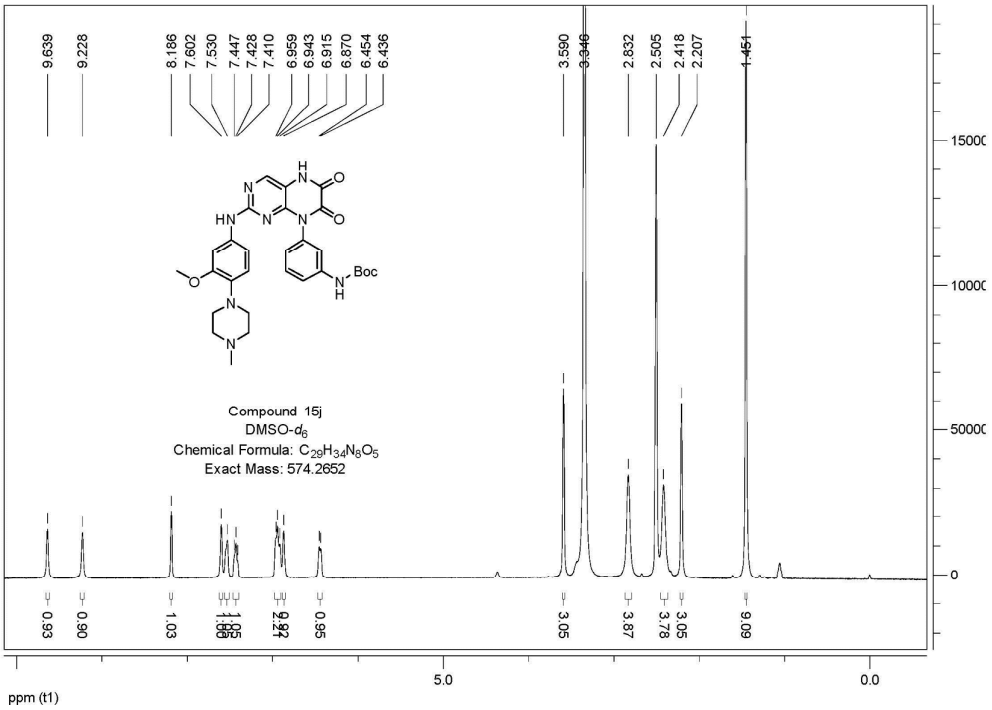
9.639
9.228
8.186
7.602
7.530
7.447
7.428
7.410
6.959
6.943
6.915
6.870
6.454
6.436
3.590
3.346
2.832
2.505
2.418
2.207
1.451
Compound 15j
DMSO-d_6
Chemical Formula: $C_{29}H_{34}N_8O_5$
Exact Mass: 574.2652
0.93
0.90
1.03
0.95
3.05
3.87
3.78
3.05
9.09
ppm (t1)

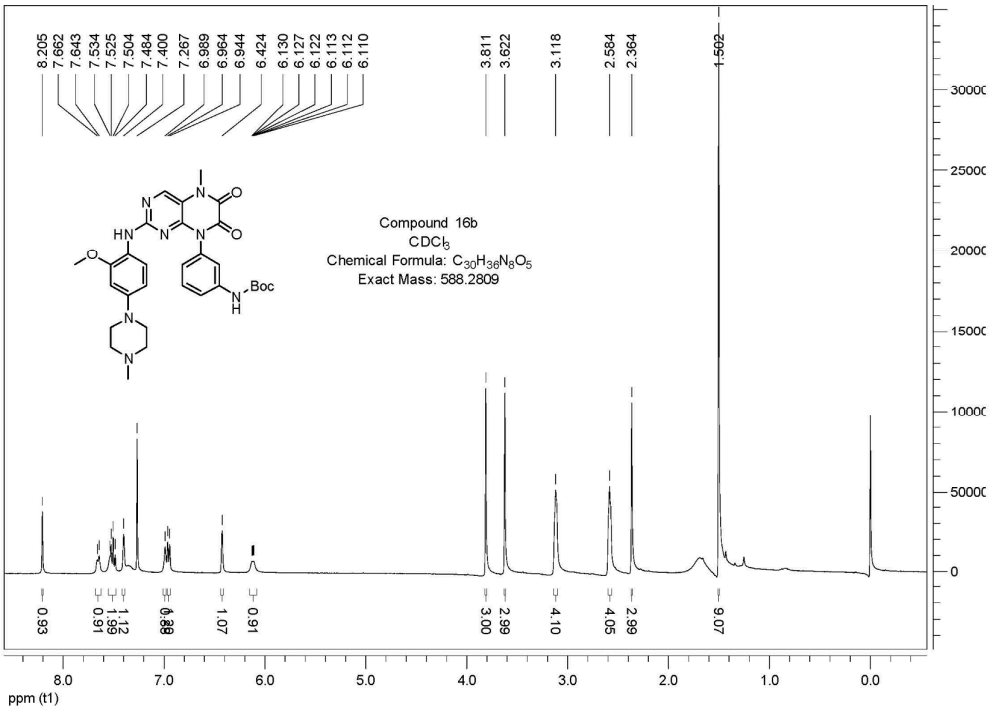
8.205
7.662
7.643
7.534
7.525
7.504
7.484
7.400
7.267
6.989
6.964
6.944
6.424
6.130
6.127
6.122
6.113
6.112
6.110
3.811
3.622
3.118
2.584
2.364
1.562
Compound 16b
$CDCl_3$
Chemical Formula: $C_{30}H_{36}N_8O_5$
Exact Mass: 588.2809
0.93
0.91
1.07
0.91
3.00
2.99
4.10
4.05
2.99
9.07
ppm (t1)

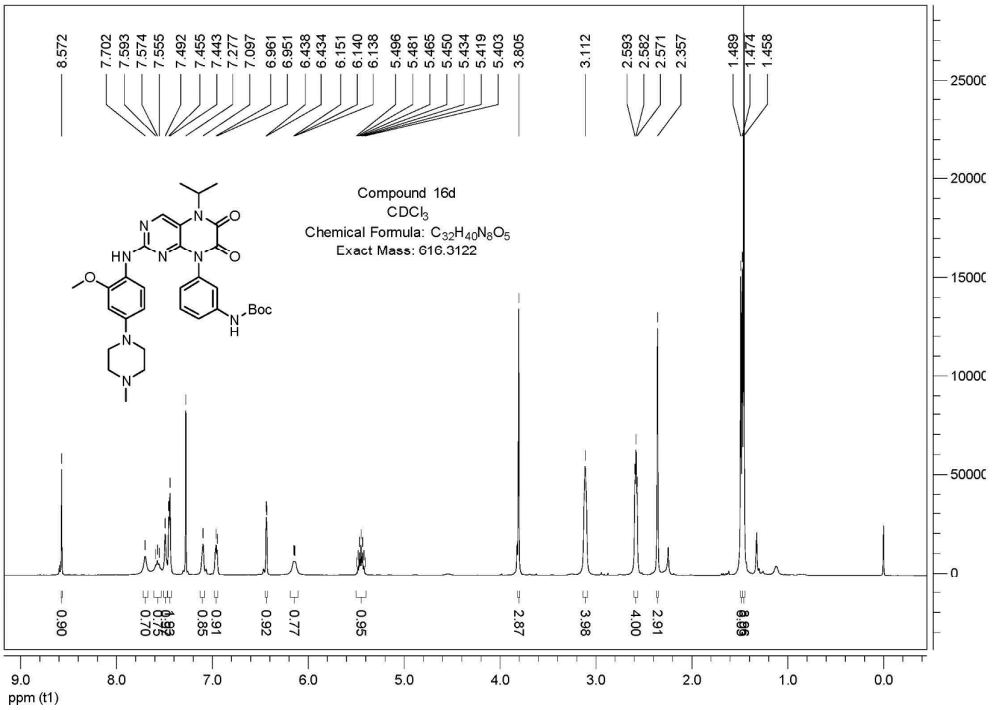
Compound 16d
CDCl3
Chemical Formula: C32H40N8O5
Exact Mass: 616.3122
Boc
ppm (t1)

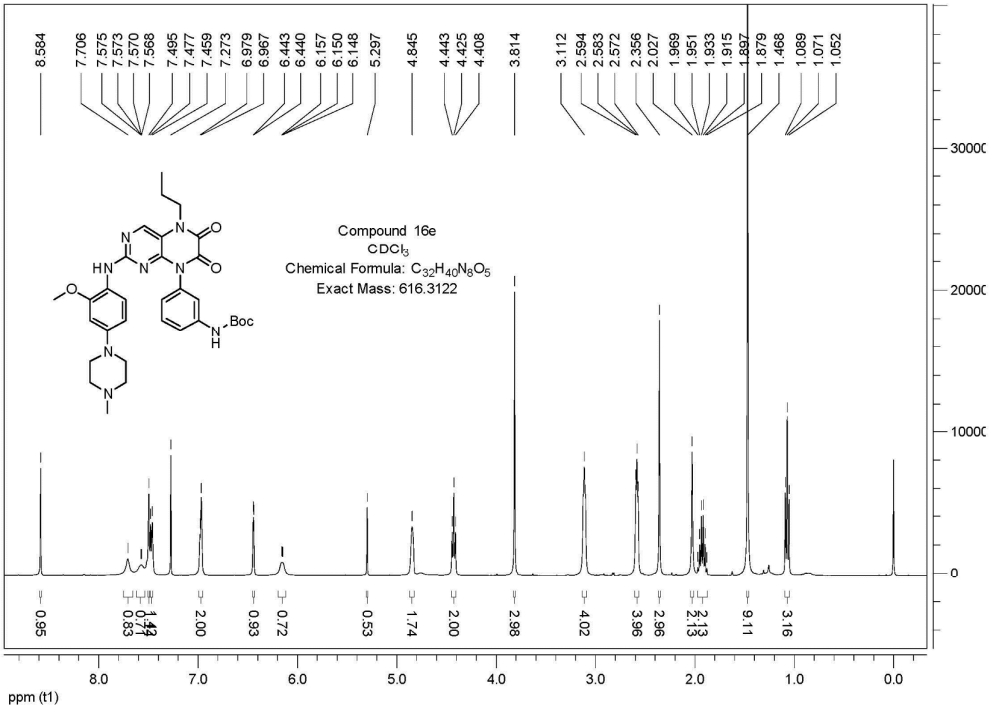
Compound 16e
CDCl3
Chemical Formula: C32H40N8O5
Exact Mass: 616.3122
Boc
ppm (t1)

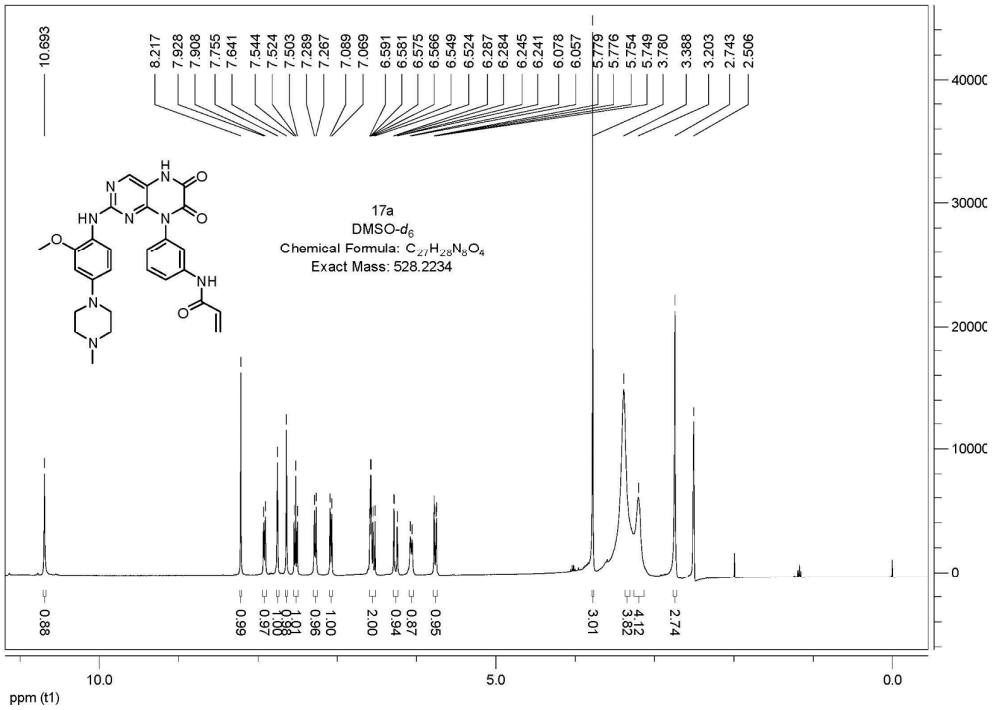
10.693
8.217
7.928
7.908
7.755
7.641
7.544
7.524
7.503
7.289
7.267
7.089
7.069
6.591
6.581
6.575
6.566
6.549
6.524
6.287
6.284
6.245
6.241
6.078
6.057
5.779
5.776
5.754
5.749
5.780
3.388
3.203
2.743
2.506
17a
DMSO-d6
Chemical Formula: C27H28N8O4
Exact Mass: 528.2234
0.88
0.99
0.67
1.01
0.96
1.00
2.00
0.94
0.87
0.95
3.01
3.92
4.12
2.74
ppm (t1)

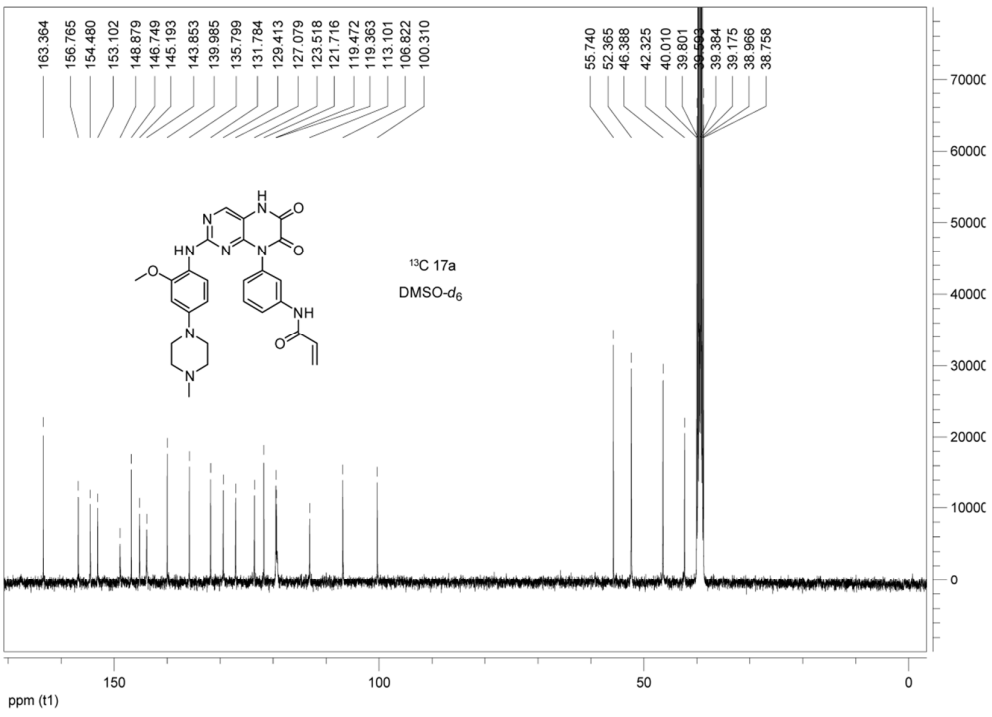
163.364
156.765
154.480
153.102
148.879
146.749
145.193
143.853
139.985
135.799
131.784
129.413
127.079
123.518
121.716
119.472
119.363
113.101
106.822
100.310
55.740
52.365
46.388
42.325
40.010
39.801
39.593
39.384
39.175
38.966
38.758
13C 17a
DMSO-d6
ppm (t1)

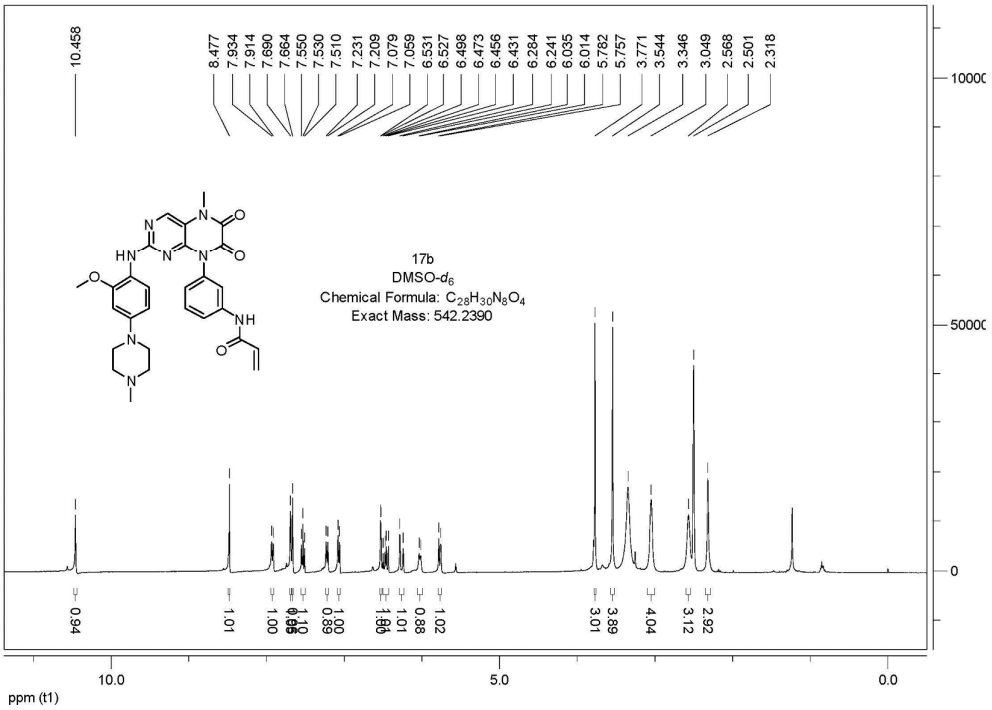
10.458
8.477
7.934
7.914
7.690
7.664
7.550
7.530
7.510
7.231
7.209
7.079
7.059
6.531
6.527
6.498
6.473
6.456
6.431
6.284
6.241
6.035
6.014
5.782
5.757
3.771
3.544
3.346
3.049
2.568
2.501
2.318
17b
DMSO-d_6
Chemical Formula: $C_{28}H_{30}N_8O_4$
Exact Mass: 542.2390
0.94
1.01
1.00
0.89
1.00
1.01
0.88
1.02
3.01
3.89
4.04
3.12
2.92
10.0
5.0
0.0
ppm (t1)

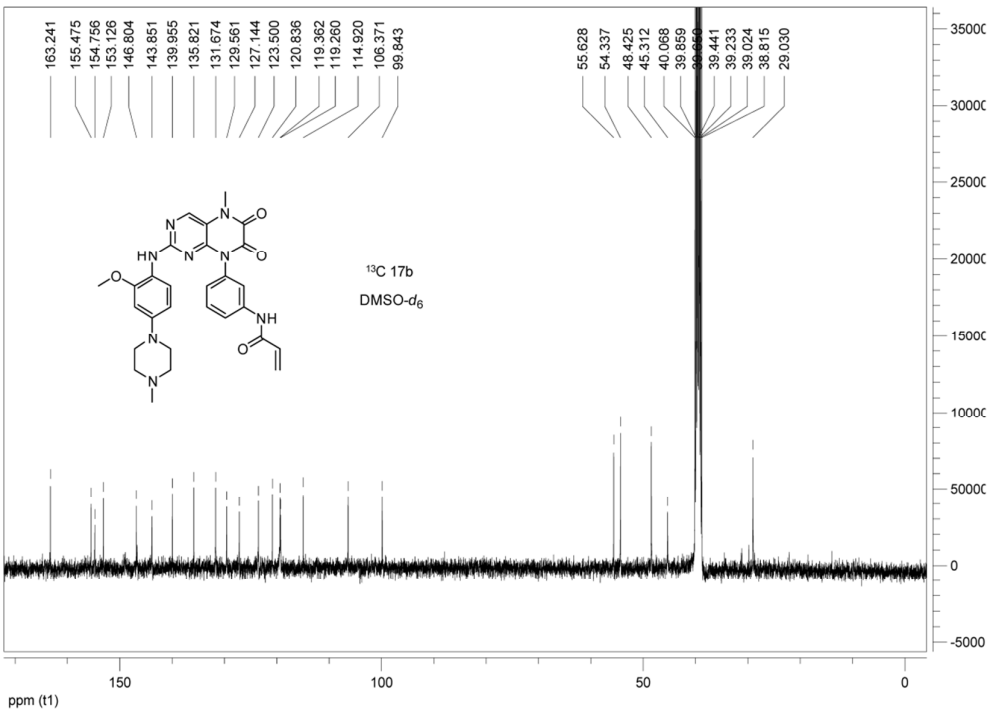
163.241
155.475
154.756
153.126
146.804
143.851
139.955
135.821
131.674
129.561
127.144
123.500
120.836
119.362
119.260
114.920
106.371
99.843
55.628
54.337
48.425
45.312
40.068
39.859
39.441
39.233
39.024
38.815
29.030
^{13}C 17b
DMSO-d_6
150
100
50
0
ppm (t1)

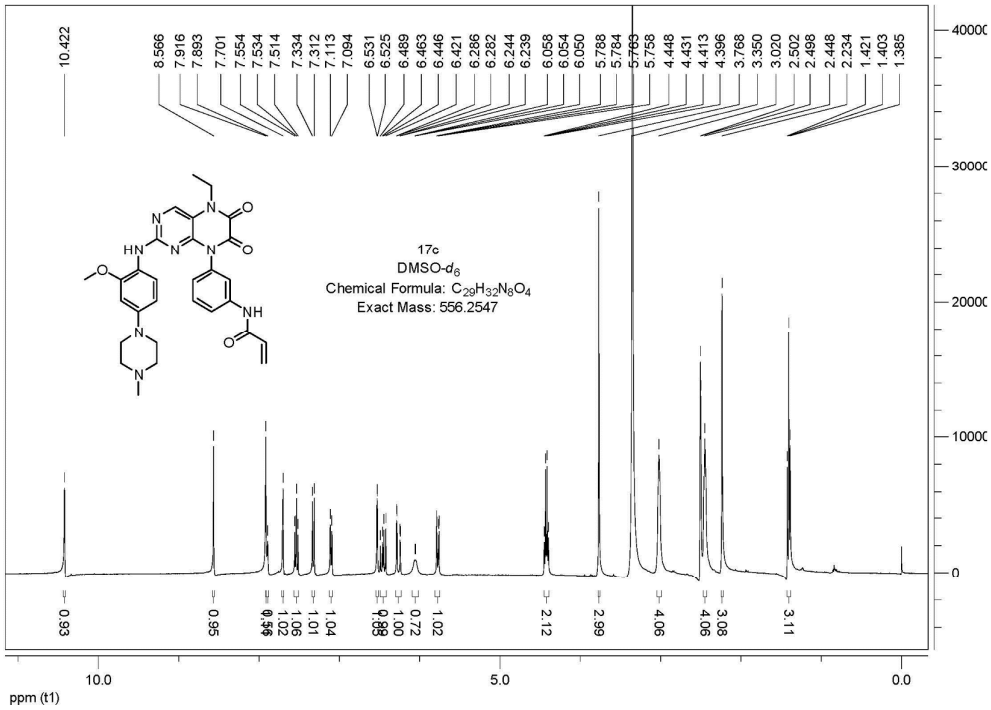
10.422
8.566
7.916
7.893
7.701
7.554
7.534
7.514
7.334
7.312
7.113
7.094
6.531
6.525
6.489
6.463
6.446
6.421
6.286
6.282
6.244
6.239
6.058
6.054
6.050
5.788
5.784
5.763
5.758
4.448
4.431
4.413
4.396
3.768
3.350
3.020
2.502
2.498
2.448
2.234
1.421
1.403
1.385
17c
DMSO-d_6
Chemical Formula: $C_{29}H_{32}N_8O_4$
Exact Mass: 556.2547
0.93
0.95
1.02
1.06
1.01
1.04
1.00
0.72
1.02
2.12
2.99
4.06
4.06
3.08
3.11
10.0
5.0
0.0
ppm (t1)

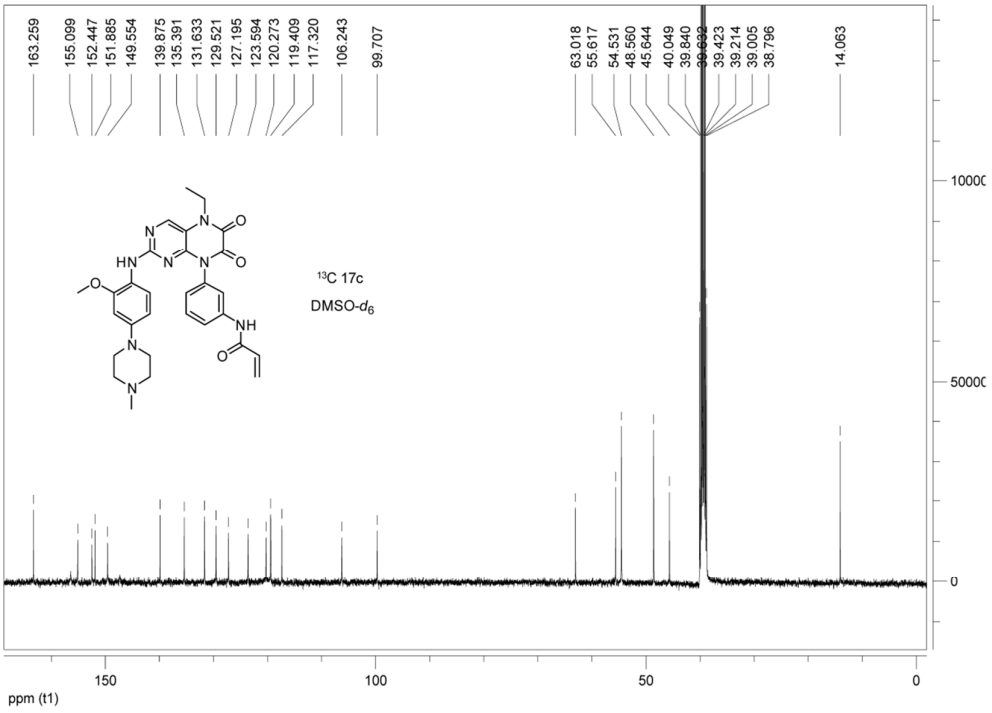
163.259
155.099
152.447
151.885
149.554
139.875
135.391
131.633
129.521
127.195
123.594
120.273
119.409
117.320
106.243
99.707
63.018
55.617
54.531
48.560
45.644
40.049
39.840
39.423
39.214
39.005
38.796
14.063
^{13}C 17c
DMSO-d_6
150
100
50
0
ppm (t1)

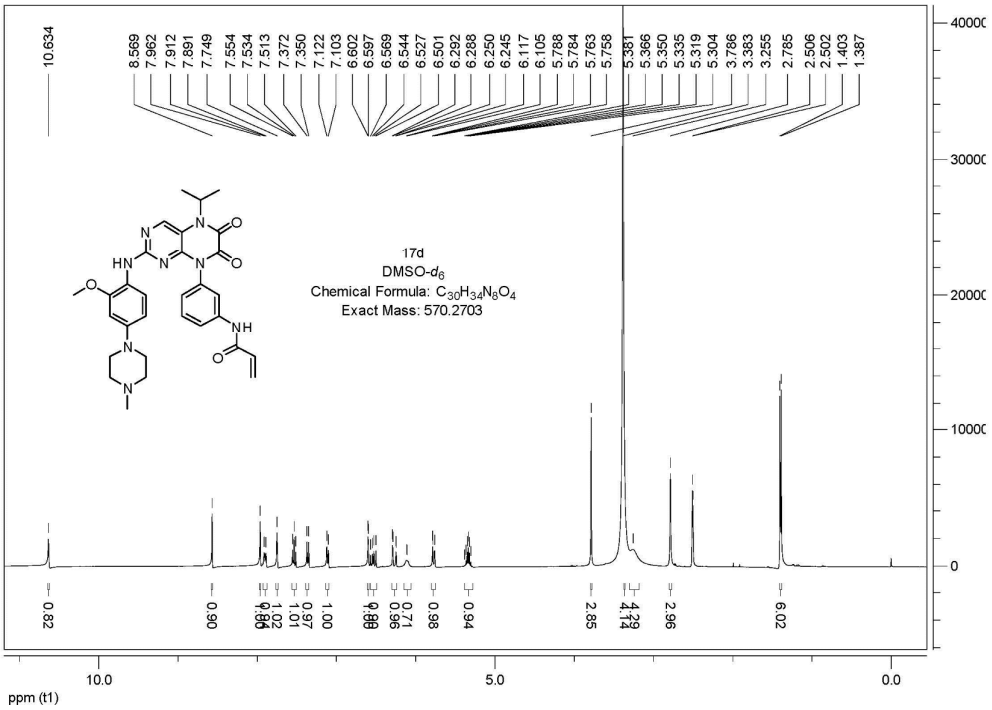
10.634
8.569
7.962
7.912
7.891
7.749
7.554
7.534
7.513
7.372
7.350
7.122
7.103
6.602
6.597
6.569
6.544
6.527
6.501
6.292
6.288
6.250
6.245
6.117
6.105
5.788
5.784
5.763
5.758
5.381
5.366
5.350
5.335
5.319
5.304
3.786
3.383
3.255
2.785
2.506
2.502
1.403
1.387
17d
DMSO-d6
Chemical Formula: C30H34N8O4
Exact Mass: 570.2703
0.82
0.90
1.00
0.71
0.98
0.94
2.85
4.14
2.96
9.02
10.0
5.0
0.0
ppm (t1)

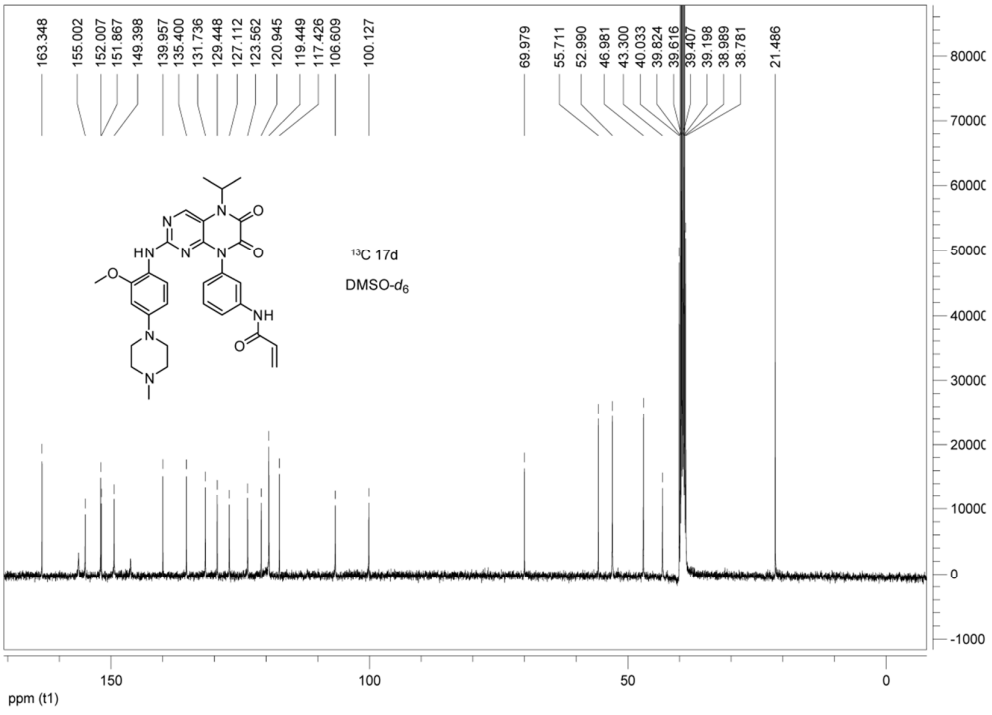
163.348
155.002
152.007
151.867
149.398
139.957
135.400
131.736
129.448
127.112
123.562
120.945
119.449
117.426
106.609
100.127
69.979
55.711
52.990
46.981
43.300
40.033
39.824
39.616
39.407
39.198
38.989
38.781
21.486
13C 17d
DMSO-d6
150
100
50
0
ppm (t1)

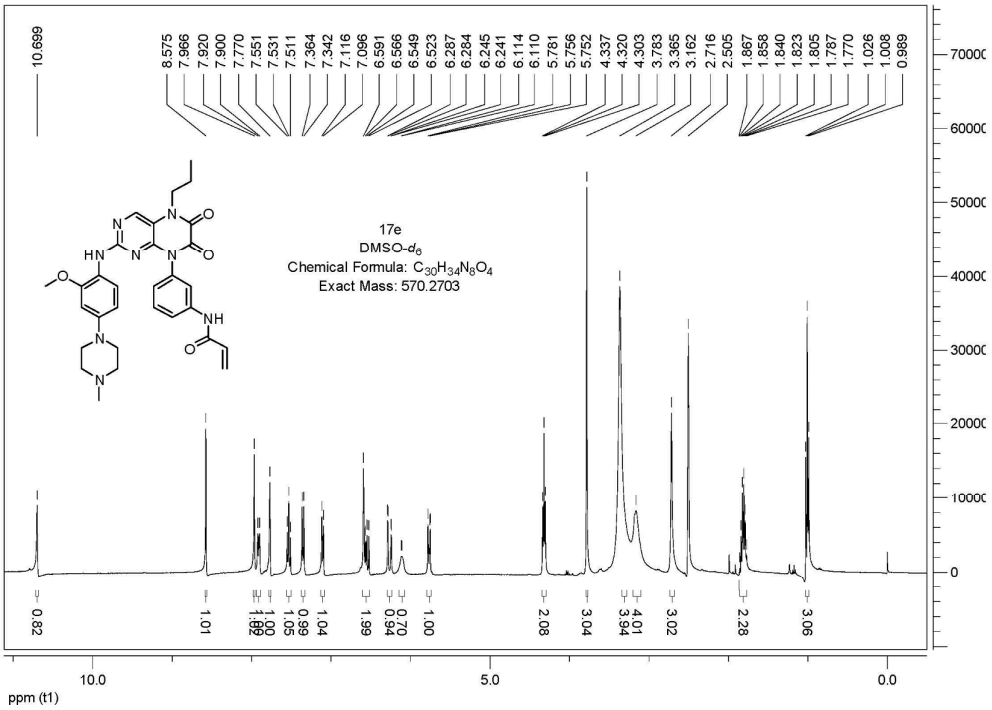
17e
DMSO-d_6
Chemical Formula: $C_{30}H_{34}N_8O_4$
Exact Mass: 570.2703
ppm (t1)

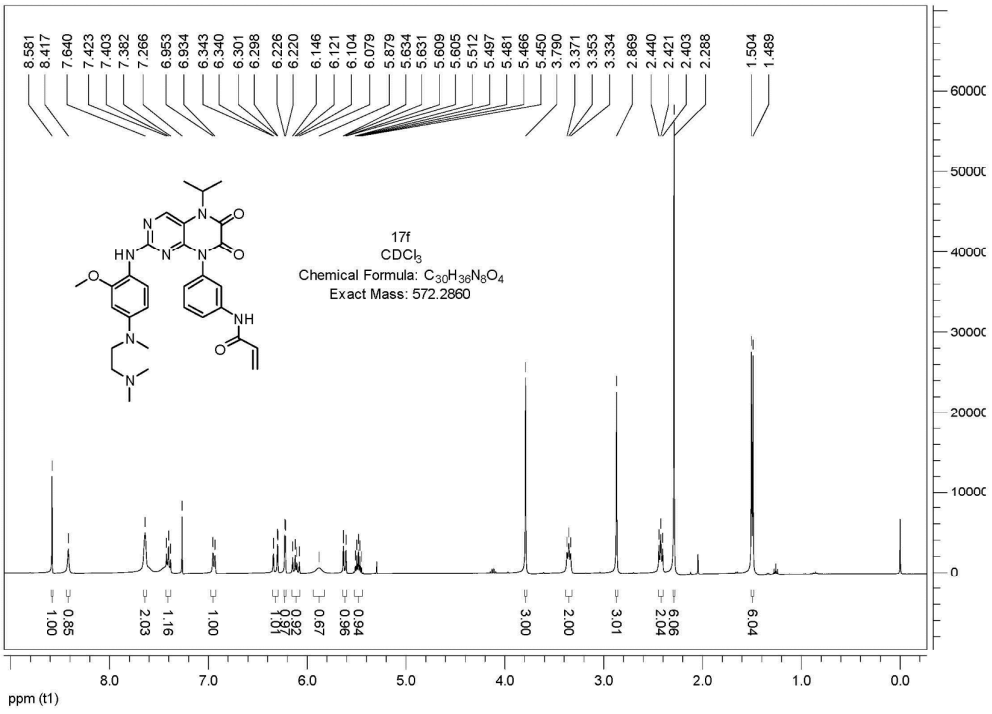
17f
$CDCl_3$
Chemical Formula: $C_{30}H_{36}N_8O_4$
Exact Mass: 572.2860
ppm (t1)

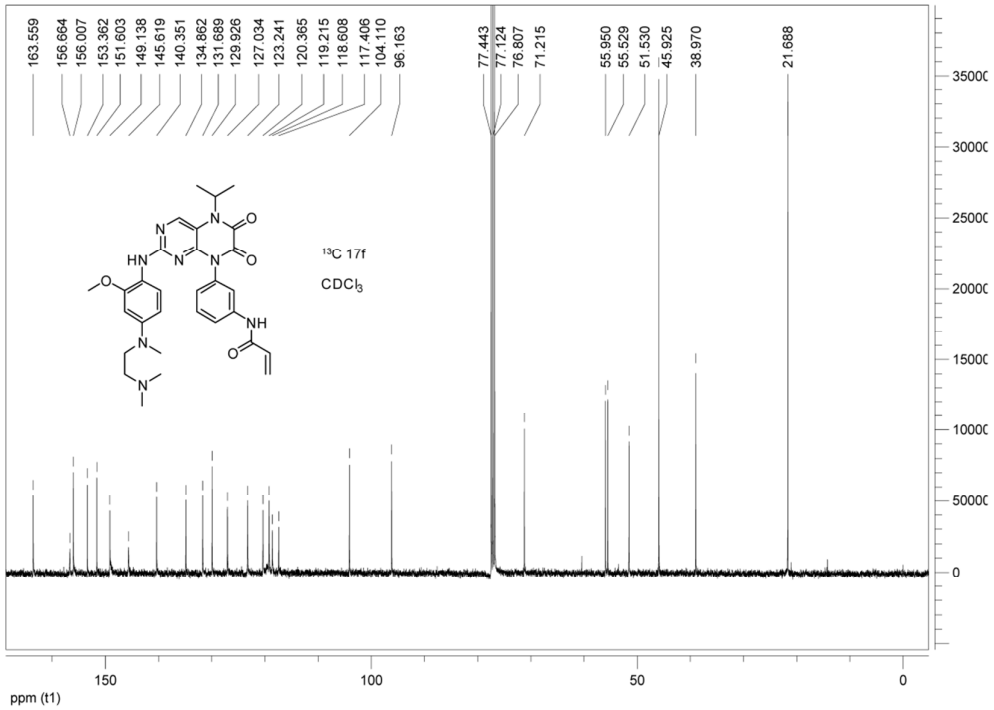
163.559
156.664
156.007
153.362
151.603
149.138
145.619
140.351
134.862
131.689
129.926
127.034
123.241
120.365
119.215
118.608
117.406
104.110
96.163
77.443
77.124
76.807
71.215
55.950
55.529
51.530
45.925
38.970
21.688
^{13}C 17f
$CDCl_3$
ppm (t1)

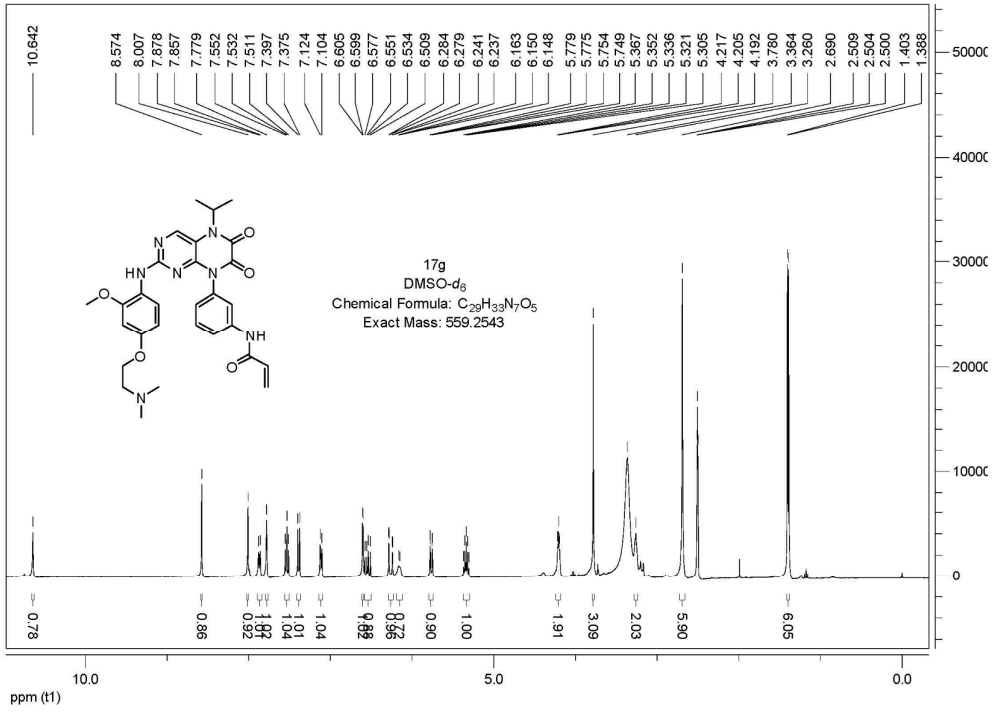
10.642
8.574
8.007
7.878
7.857
7.779
7.552
7.532
7.511
7.397
7.375
7.124
7.104
6.605
6.599
6.577
6.551
6.534
6.509
6.284
6.279
6.241
6.237
6.163
6.150
6.148
5.779
5.775
5.754
5.749
5.367
5.352
5.336
5.321
5.305
4.217
4.205
4.192
3.780
3.364
3.260
2.690
2.509
2.504
2.500
1.403
1.388
17g
DMSO-d_6
Chemical Formula: $C_{29}H_{33}N_7O_5$
Exact Mass: 559.2543
0.78
0.86
0.92
1.02
1.01
1.04
1.04
0.90
1.00
1.91
3.09
2.03
5.90
6.05
ppm (t1)

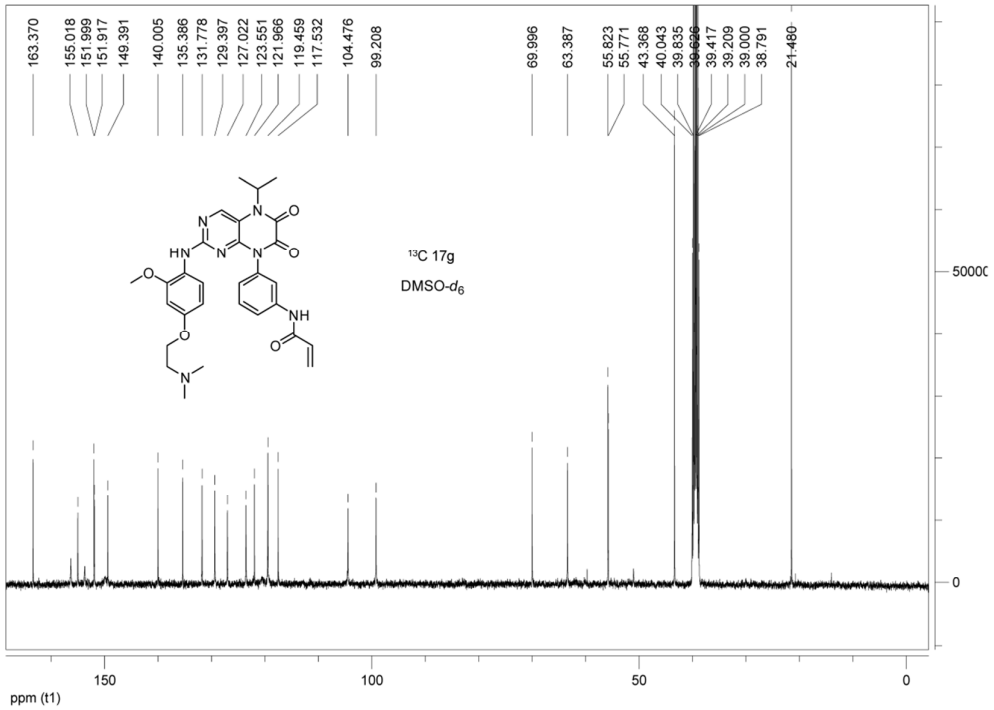
163.370
155.018
151.999
151.917
149.391
140.005
135.386
131.778
129.397
127.022
123.551
121.966
119.459
117.532
104.476
99.208
69.996
63.387
55.823
55.771
43.368
40.043
39.835
39.417
39.209
39.000
38.791
21.480
^{13}C 17g
DMSO-d_6
5000
0
150
100
50
0
ppm (t1)

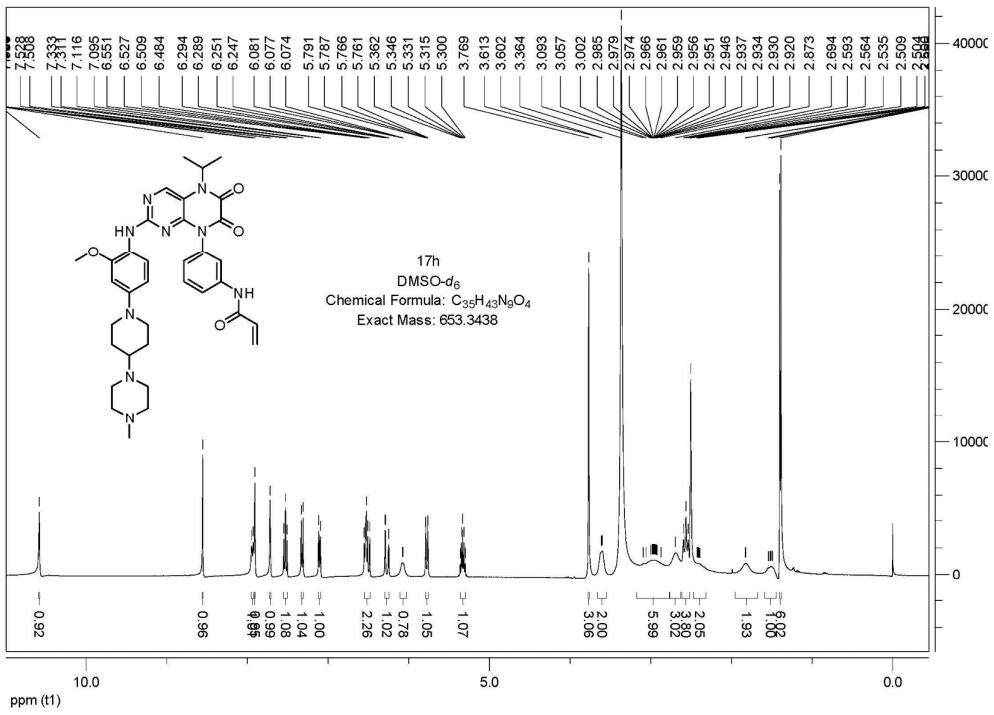
17h
DMSO-d_6
Chemical Formula: $C_{35}H_{43}N_9O_4$
Exact Mass: 653.3438
4000
3000
2000
1000
0
0.92
0.96
0.90
1.00
2.26
1.05
1.07
3.96
2.00
5.99
1.93
10.0
5.0
0.0
ppm (t1)

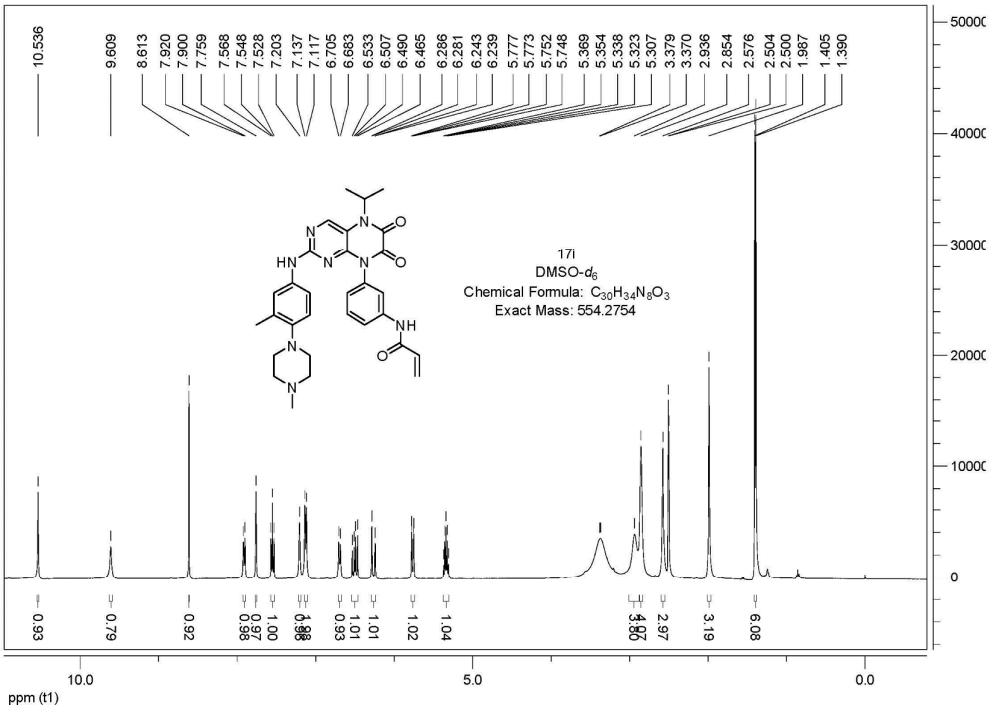
10.536
9.609
8.613
7.920
7.900
7.759
7.568
7.548
7.528
7.203
7.137
7.117
6.705
6.683
6.533
6.507
6.490
6.465
6.286
6.281
6.243
6.239
5.777
5.773
5.752
5.748
5.369
5.354
5.338
5.323
5.307
3.379
3.370
2.936
2.854
2.576
2.504
2.500
1.987
1.405
1.390
17i
DMSO-d_6
Chemical Formula: $C_{30}H_{34}N_8O_3$
Exact Mass: 554.2754
0.93
0.79
0.92
0.98
0.97
1.00
0.93
1.01
1.01
1.02
1.04
3.80
2.97
3.19
9.08
10.0
5.0
0.0
ppm (t1)

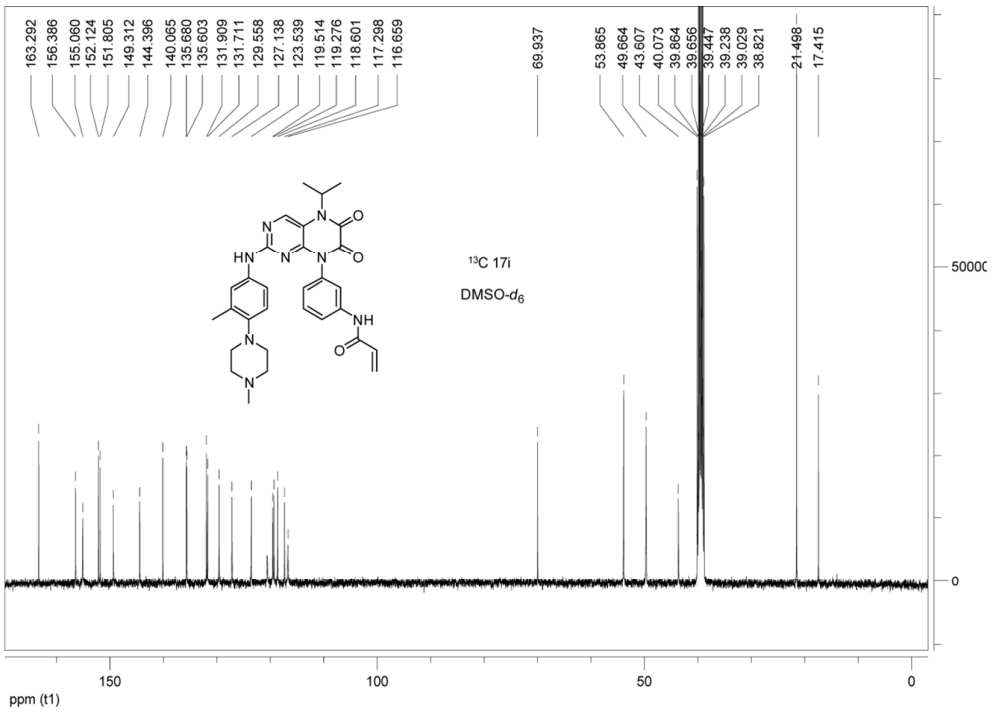
163.292
156.386
155.060
152.124
151.805
149.312
144.396
140.065
135.680
135.603
131.909
131.711
129.558
127.138
123.539
119.514
119.276
118.601
117.298
116.659
69.937
53.865
49.664
43.607
40.073
39.864
39.656
39.447
39.238
39.029
38.821
21.498
17.415
^{13}C 17i
DMSO-d_6
150
100
50
0
ppm (t1)

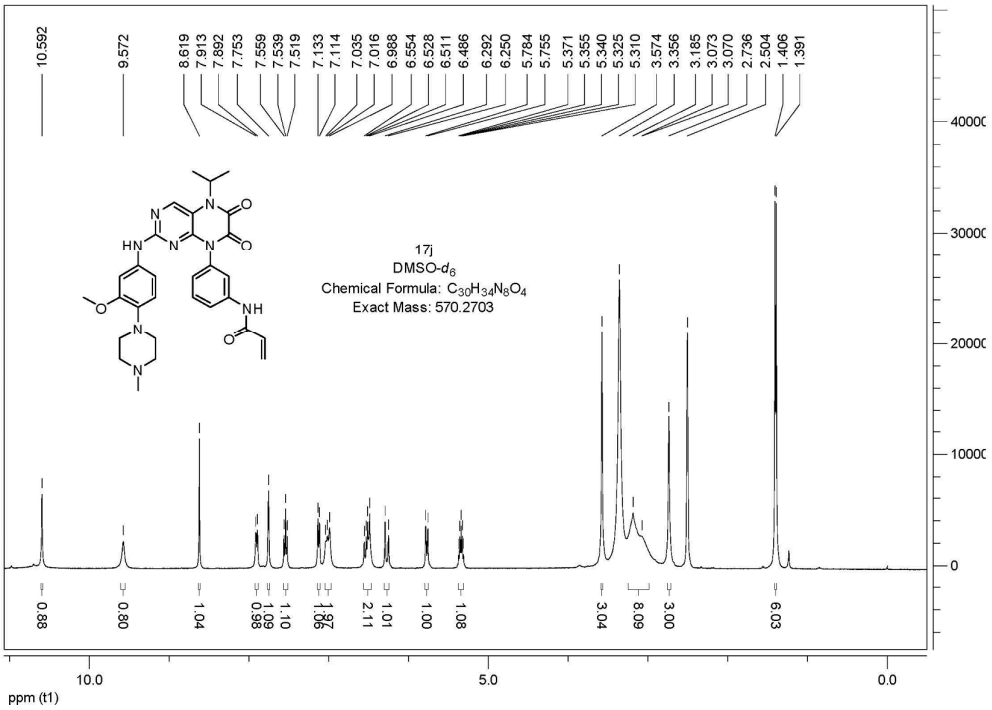
10.592
9.572
8.619
7.913
7.892
7.753
7.559
7.539
7.519
7.133
7.114
7.035
7.016
6.988
6.554
6.528
6.511
6.486
6.292
6.250
5.784
5.755
5.371
5.355
5.340
5.325
5.310
3.574
3.356
3.185
3.073
3.070
2.736
2.504
1.406
1.391
17j
DMSO-d_6
Chemical Formula: $C_{30}H_{34}N_8O_4$
Exact Mass: 570.2703
0.88
0.80
1.04
0.98
1.09
1.10
1.96
1.87
2.11
1.01
1.00
1.08
3.04
8.69
3.00
6.03
10.0
5.0
0.0
ppm (t1)

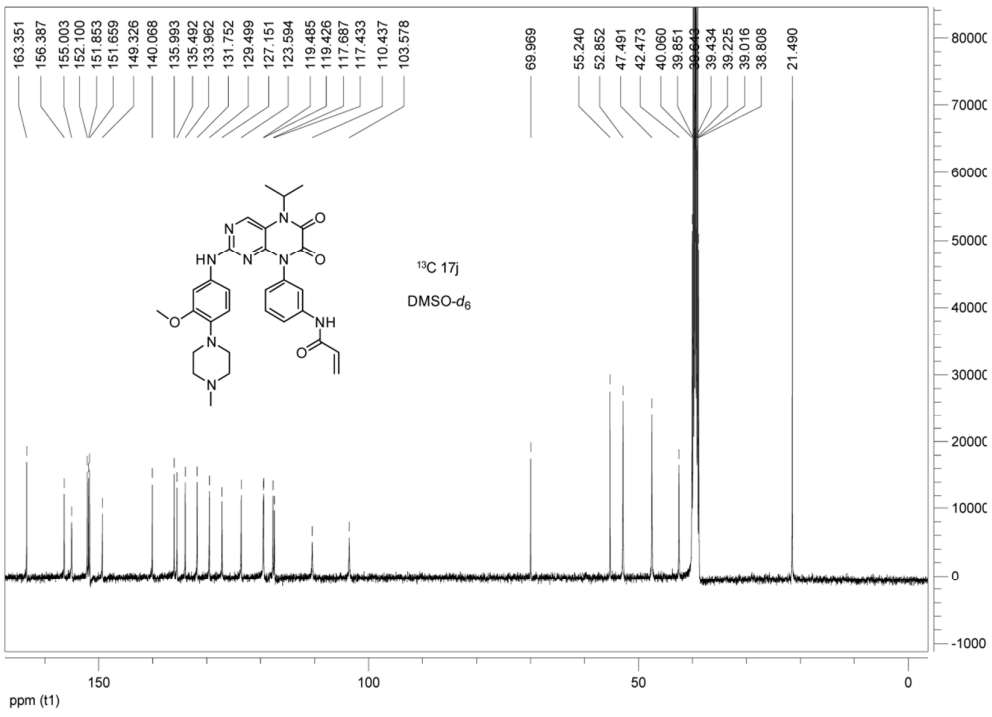
163.351
156.387
155.003
152.100
151.853
151.659
149.326
140.068
135.993
135.492
133.962
131.752
129.499
127.151
123.594
119.485
119.426
117.687
117.433
110.437
103.578
69.969
55.240
52.852
47.491
42.473
40.060
39.851
39.642
39.434
39.225
39.016
38.808
21.490
^{13}C 17j
DMSO-d_6
150
100
50
0
ppm (t1)

REFERENCES

(1) Liu, X.; Jiang, H.; Li, H. SHAFTS: A Hybrid Approach for 3D Molecular Similarity Calculation. 1. Method and Assessment of Virtual Screening. *J. Chem. Inf. Model.* **2011,** *51*, 2372-2385.
(2) Liu, X.; Bai, F.; Ouyang, S.; Wang, X.; Li, H.; Jiang, H. Cyndi: A multi-objective evolution algorithm based method for bioactive molecular conformational generation. *BMC Bioinformatics* **2009,** *10*, 101.
(3) Zhou, W.; Ercan, D.; Chen, L.; Yun, C.; Li, D.; Capelletti, M.; Cortot, A. B.; Chirieac, L.; Iacob, R. E.; Padera, R.; Engen, J. R.; Wong, K.; Eck, M. J.; Gray, N. S.; Jänne, P. A. Novel Mutant-Selective EGFR Kinase Inhibitors against EGFR T790M. *Nature* **2009,** *462*, 1070-1074.
(4) Gong J.; Cai C.; Liu X.; Ku X.; Jiang H.; Gao D.; Li H. ChemMapper: A Versatile Web Server for Exploring Pharmacology and Chemical Structure Association Based on Molecular 3D Similarity Method. *Bioinformatics* **2013,** *29*, 1827-1829.
(5) Solca, F.; Dahl, G.; Zoephel, A.; Bader, G.; Sanderson, M.; Klein, C.; Kraemer, O.; Himmelsbach, F.; Haaksma, E.; Adolf, G. R. Target Binding Properties and Cellular Activity of Afatinib (BIBW2992), an Irreversible ErbB Family Blocker. *J. Pharmacol. Exp. Ther.* **2012**, *343*, 342-350.
(6) Friesner, R.; Banks, J.; Murphy, R.; Halgren, T.; Klicic, J.; Mainz, D.; Repasky, M.; Knoll, E.; Shelley, M.; Perry, J. Glide: a new approach for rapid, accurate docking and scoring. 1. Method and assessment of docking accuracy. *J. Med. Chem.* **2004,** *47(7)*, 1739−1749.
(7) Ghomsi, N. T.; Ahabchane, N. E. H.; Es-Safi, N. E.; Garrigues, B.; Essassi, E. M. Synthesis and Spectroscopic Structural Elucidation of New Quinoxaline Derivatives. *Spectrosc. Lett.* **2007,** *40*, 741-751.